ISSN 1674-1056
http://cpb.iphy.ac.cn
http://iopscience.iop.org/cpb
中国物理 B
Chinese Physics
中国物理
Chinese Physics B

Axial acoustic radiation force on a fluid sphere between two impedance boundaries for Gaussian beam

Yuchen Zang(臧雨宸), Yupei Qiao(乔玉配), Jiehui Liu(刘杰惠), Xiaozhou Liu(刘晓宙)

Citation: Chin. Phys. B . 2019, 28(3): 034301. **doi:** 10.1088/1674-1056/28/3/034301
Journal homepage: http://cpb.iphy.ac.cn; http://iopscience.iop.org/cpb

What follows is a list of articles you may be interested in

Acoustic radiation force on a multilayered sphere in a Gaussian standing field

Haibin Wang(汪海宾), Xiaozhou Liu(刘晓宙), Sha Gao(高莎), Jun Cui(崔骏), Jiehui Liu(刘杰惠), Aijun He(何爱军), Gutian Zhang(张古田)

Chin. Phys. B . 2018, 27(3): 034302. **doi:** 10.1088/1674-1056/27/3/034302

Random phase screen influence of the inhomogeneous tissue layer on the generation of acoustic vortices

Zhiyao Ma(马致遥), Jun Ma(马骏), Dong Zhang(章东), Juan Tu(屠娟)

Chin. Phys. B . 2018, 27(3): 034301. **doi:** 10.1088/1674-1056/27/3/034301

Multiple off-axis acoustic vortices generated by dual coaxial vortex beams

Wen Li(李雯), Si-Jie Dai(戴思捷), Qing-Yu Ma(马青玉), Ge-Pu Guo(郭各朴), He-Ping Ding(丁鹤平)

Chin. Phys. B . 2018, 27(2): 024301. **doi:** 10.1088/1674-1056/27/2/024301

Acoustic radiation force induced by two Airy-Gaussian beams on a cylindrical particle

Sha Gao(高莎), Yiwei Mao(毛一葳), Jiehui Liu(刘杰惠), Xiaozhou Liu(刘晓宙)

Chin. Phys. B . 2018, 27(1): 014302. **doi:** 10.1088/1674-1056/27/1/014302

Tunable acoustic radiation pattern assisted by effective impedance boundary

Feng Qian(钱 枫), Li Quan(全力), Li-Wei Wang(王力维), Xiao-Zhou Liu (刘晓宙), Xiu-Fen Gong(龚秀芬)

Chin. Phys. B . 2016, 25(2): 024301. **doi:** 10.1088/1674-1056/25/2/024301

Axial acoustic radiation force on a fluid sphere between two impedance boundaries for Gaussian beam*

Yuchen Zang(臧雨宸)[1], Yupei Qiao(乔玉配)[1], Jiehui Liu(刘杰惠)[1], and Xiaozhou Liu(刘晓宙)[1,2,†]

[1] *Key Laboratory of Modern Acoustics, Institute of Acoustics and School of Physics, Collaborative Innovation Center of Advanced Microstructures, Nanjing University, Nanjing* 210093, *China*

[2] *Key Laboratory of Acoustics, Institute of Acoustics, Chinese Academy of Sciences, Beijing* 100190, *China*

(Received 14 December 2018; revised manuscript received 15 January 2019; published online 22 February 2019)

The acoustic radiation force on a fluid sphere immersed in water between two boundaries given by a Gaussian beam is theoretically and numerically investigated in this work. Based on the finite series method, the Gaussian beam is expressed in terms of Bessel function and a weighting parameter. The effects of the two boundaries concerned in our study is worked out by the image theory. This work also provides a reference when considering the effects of certain factors such as the radius of the sphere and the distance between the sphere and two boundaries. The contrast with the acoustic radiation force on a fluid sphere near only one boundary is also made in this paper. Our study can offer a theoretical basis for acoustics manipulation, acoustic sensors in the field of biomedical ultrasound and material science.

Keywords: acoustic radiation force, Gaussian beam, fluid sphere, impedance boundary

PACS: 43.25.Qp, 43.35.Wa, 43.80.Gx **DOI:** 10.1088/1674-1056/28/3/034301

1. Introduction

The acoustic radiation force is derived from the nonlinear effect of acoustic waves. Usually, the force is so weak that it is often neglected. But when the intensity of sound reaches a relatively high degree, it cannot be overlooked. Due to its widespread applications in many fields, a variety of theoretical and experimental studies about acoustics radiation force acting on spherical and cylindrical particles have been conducted.[1–6] For example, King, who first set forth the concept of the acoustic radiation force on particles, provided a theoretical model of the acoustic radiation force on a sphere in 1934.[4] Awatani first successfully calculated the acoustic radiation force on a rigid cylinder.[7] In 1955, Yosioka considered the acoustic radiation force on a compressible sphere and discussed about various factors that affected the results in details.[6] Shortly after, the acoustic radiation force acting on elastic particles were given by Hasagawa,[8] who also studied the acoustic radiation force on a sphere in a quasistationary wave field.[9] More recently, Azarpeyv and Yosioka have investigated the acoustic radiation force on a rigid cylinder in the Gaussian beam field using finite series method.[10] Some scientists also further considered the arbitrarily placed particles in focused Gaussian beam. The acoustic radiation force acting on a cylinder near one boundary in a plane wave field was figured out by Zhang's group.[11] Later, they also completed the radiation force exerted by axial Gaussian beam in the same case.[12] On top of that, acoustic scattering on a spherical body near a plane boundary was analyzed by Gaunaurd and Huang.[13] Miri worked out the acoustic radiation force on a spherical shell near a vessel porous wall.[14]

Nevertheless, none of these studies has touched on the acoustic radiation force on particles between two impedance boundaries, which is often considered in many biomedical ultrasound applications, especially drug delivery in vessels. Early researches mainly focused on the acoustic radiation force in the plane wave field. However, the Gaussian beam is widely used in biomedical ultrasound and material engineering, especially with the rapid development of the ultrasonic transducer nowadays. In this study, we analyze the acoustic radiation force on a sphere between two impedance boundaries. Moreover, we also discuss how the property of the sphere as well as the distance between the particle and the boundaries affects the force. Several numerical simulations are also given in this work to achieve a cross reference with our theoretical analysis.

2. Theory

A fluid spherical particle with radius a is positioned in an on-axis Gaussian beam with the beam waist W_0. The propagation direction of the wave is along the $+z$ direction, which is perpendicular to the two parallel placed impedance boundaries. The distances between the sphere and the two boundaries are d_1 and d_2, respectively. The origin O of a spherical coordinate system (r, θ) coincides with the center of the

*Project supported by the National Key Research and Development Program of China (Grant No. 2016YFF0203000), State Key Program of National Natural Science of China (Grant No. 11834008), National Natural Science Foundation of China (Grant No. 11774167), State Key Laboratory of Acoustics, Chinese Academy of Science (Grant No. SKLA201809), and Administration of Quality Supervision, Inspection and Quarantine (AQSIQ) Technology Research and Development Program, China (Grant No. 2017QK125).

†Corresponding author. E-mail: xzliu@nju.edu.cn

© 2019 Chinese Physical Society and IOP Publishing Ltd

sphere. The schematic diagram of the problem is shown in Fig. 1. The image theory can be employed to analyze the effect of the impedance boundaries on the acoustic radiation force here.

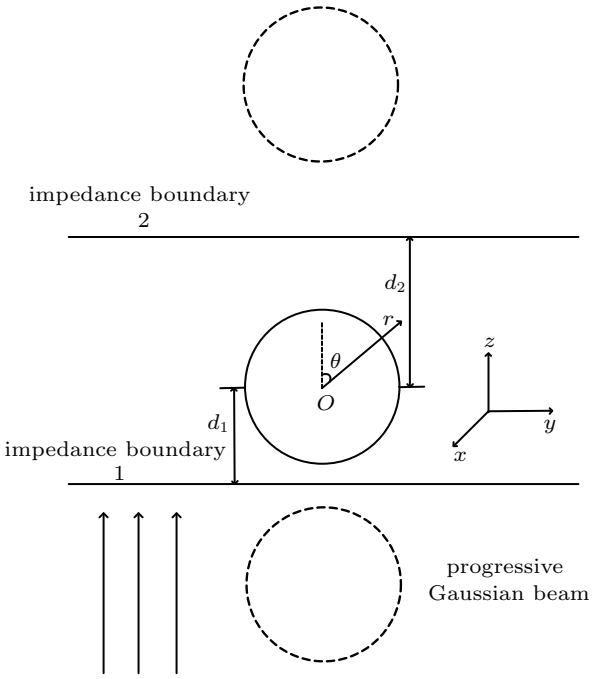


Fig. 1. The schematic diagram of the problem.

Two images of the sphere are set respectively above the half-boundary line, which are of the exact same size as the real sphere. Theoretically, an infinite number of images should be introduced to be equivalent to the two boundaries. However, as for other images, the distances between the fluid spherical particle and the images are increasing so significantly that the influence of the images on acoustic radiation force can be ignored. The distances between the centers of images and their corresponding boundary are also d_1 and d_2, respectively. It is important to note that d_1 and d_2 are opposite in their signs because the two boundaries are on opposite sides of the sphere.

The origin of each image coordinate systems is set at the center of the image sphere, respectively. The reflections of the incident wave by the boundaries are two image incident waves of the same magnitude but opposite directions. In addition, the reflections of the scattering wave are regarded as the scattering waves from the image spheres.

2.1. Expansion of incident Gaussian beam in terms of spherical functions

Assuming that the fluid in which the wave travels is non-viscous, the wave equation can be written as

$$\left(\nabla^2 + k^2\right)\phi = 0, \tag{1}$$

where ϕ is the total velocity potential, and k is the wave number in the fluid medium.

We can derive the general approximation of a Gaussian beam through replacing the original Helmholtz equation with the parabolic differential equation[15,16]

$$\phi_{\text{inc}} = \phi_0 \left(1 - \mathrm{i}\frac{z}{b}\right)^{-1} \mathrm{e}^{-\mathrm{i}kz - \mathrm{i}k\frac{x^2+y^2}{2r_{\text{wf}}} - \frac{x^2+y^2}{L^2}} \mathrm{e}^{-\mathrm{i}\omega t}, \tag{2}$$

$$L = L_0 \left[1 + \left(\frac{z}{b}\right)\right]^{1/2}, \tag{3}$$

where ϕ_{inc} is the velocity potential of incident wave whose amplitude is ϕ_0, x, y, and z represent the location in the coordinate system, $L_0 = kW_0^2$ determines the size of the focused beam, $b = kL_0^2/2$, and $r_{\text{wf}} = z + b^2/z$ represents the local radius of curvature of the equiphase near the beam axis.

It is not difficult to find that the value of kL_0 determines the rate of its spreading. When z/b is small, spreading is sometimes locally ignored and a three-dimensional Gaussian beam can be simplified locally to the following expression:

$$\phi_{\text{inc}} = \phi_0 \mathrm{e}^{-\left(\frac{x^2+y^2}{L_0^2}\right)} \mathrm{e}^{-\mathrm{i}kz} \mathrm{e}^{-\mathrm{i}\omega t}, \tag{4}$$

where ω is the angular frequency.

There are some other reasons why we should set z to be relatively small. With the increase of the distance from the focal plane, we cannot ignore several effects caused by the propagation.[17] In Ref. [17], figures 2 and 3 show us how the scaled amplitude and phase change with different values of z. Inspection of these figures tells us that we can only ignore the evolution of amplitude and phase at small distance. Based on this conclusion, all of our calculation and discussion is limited to the vicinity of the focal plane. Meanwhile, the distance between two parallel planes must also satisfy $h = d_1 + d_2 \ll b$. According to the theory of finite series expansion, it can be expanded in the spherical coordinate system as[12]

$$\phi_{\text{inc}} = \phi_0 \mathrm{e}^{-\mathrm{i}\omega t} \sum_{n=0}^{\infty} (2n+1)\, g_n \mathrm{i}^n j_n(kr) P_n(\cos\theta), \tag{5}$$

where $z = r\cos\theta$, $x = r\sin\theta\cos\phi$, $y = r\sin\theta\sin\phi$, and g_n is the expansion coefficient of an on-axis Gaussian beam, which can be presented as[12]

$$g_n = \frac{\Gamma\left(\frac{n+1}{2}\right)}{\Gamma\left(\frac{n}{2}+1\right)} \sum_{q=0}^{\frac{n-1}{2}} \frac{\Gamma\left(\frac{n}{2}+q+1\right)}{\left(\frac{n-1}{2}-q\right)!q!} \left(-4s^2\right)^q, \text{ when } n \text{ is even},$$

$$g_n = \frac{\Gamma\left(\frac{n}{2}+1\right)}{\Gamma\left(\frac{n+1}{2}\right)} \sum_{q=0}^{\frac{n}{2}} \frac{\Gamma\left(\frac{n}{2}+q+\frac{1}{2}\right)}{\left(\frac{n}{2}-q\right)!q!} \left(-4s^2\right)^q, \text{ when } n \text{ is odd}. \tag{6}$$

Here, $s = 1/kW_0$, $j_n(\cdot)$ is the spherical Bessel function of the first kind of order n, and $P_n(\cdot)$ is the Legendre function.

2.2. Scattering of a Gaussian beam by a spherical particle between two boundaries

The reflection waves of the incident Gaussian beam from the two boundaries can be respectively expressed as

$$\phi_{\text{ref}_1} = \phi_0 \mathrm{e}^{-\mathrm{i}\omega t} \sum_{n=0}^{\infty} R_{\text{s}_1} \mathrm{e}^{\mathrm{i}2kd_1} (-1)^n$$

$$\times (2n+1)\, g_n \mathrm{i}^n j_n(kr) P_n(\cos\theta), \tag{7}$$

$$\phi_{\mathrm{ref}_2} = \phi_0 \mathrm{e}^{-\mathrm{i}\omega t} \sum_{n=0}^{\infty} R_{\mathrm{s}_2} \mathrm{e}^{\mathrm{i}2kd_2} (-1)^n \times (2n+1)\, g_n \mathrm{i}^n j_n(kr) P_n(\cos\theta), \tag{8}$$

where R_{s_1} and R_{s_2} are the acoustic reflection coefficients of the impedance boundaries respectively,[18] which can be calculated by[19]

$$R_{\mathrm{s}_i} = \frac{1-\beta_i}{1+\beta_i}, \tag{9}$$

where $\beta_i = \rho_0 c_0 / Z_i$ is the relative normal admittance of the boundary, ρ_0 and c_0 are the density and sound velocity of the fluid, respectively, and Z_i $(i = 1, 2)$ is the surface normal impedance of the media in which the image is immersed.

The scattering wave velocity potential of the fluid sphere and its image spheres can be presented as

$$\phi_{\mathrm{scat}} = \phi_0 \mathrm{e}^{-\mathrm{i}\omega t} \sum_{n=0}^{\infty} (2n+1)\, g_n \mathrm{i}^n \times a_n h_n^{(1)}(kr) P_n(\cos\theta), \tag{10}$$

$$\phi_{\mathrm{scat,ref}_1} = \phi_0 \mathrm{e}^{-\mathrm{i}\omega t} \sum_{n=0}^{\infty} R_{\mathrm{s}_1} (-1)^n (2n+1)\, g_n \mathrm{i}^n \times a_n h_n^{(1)}\left(\bar{k}\bar{r}\right) P_n\left(\cos\bar{\theta}\right), \tag{11}$$

$$\phi_{\mathrm{scat,ref}_2} = \phi_0 \mathrm{e}^{-\mathrm{i}\omega t} \sum_{n=0}^{\infty} R_{\mathrm{s}_2} (-1)^n (2n+1)\, g_n \mathrm{i}^n \times a_n h_n^{(1)}\left(\bar{k}\bar{r}\right) P_n\left(\cos\bar{\theta}\right), \tag{12}$$

where $h_n^{(1)}(\cdot)$ is the spherical Hankel function of the first kind of order n, and parameters a_n are the pending scattering coefficients left to be determined by certain boundary conditions.

The velocity potential filling in the sphere cannot be neglected when the sphere is not rigid, which can be expressed as

$$\phi_l = \phi_0 \mathrm{e}^{-\mathrm{i}\omega t} \sum_{n=0}^{\infty} (2n+1) B_n g_n \mathrm{i}^n j_n(k_l r) P_n(\cos\theta), \tag{13}$$

where k_l is the compression wave number in the fluid sphere, and B_n are the pending wave scattering coefficients to be determined by certain boundary conditions.

The most essential step to work out the acoustic radiation force is the calculation of the wave scattering coefficients. However, the velocity potentials above are expressed in different characteristic coordinate systems, making it more difficult to solve the problem. Fortunately, the spherical wave functions of the $(\bar{r}, \bar{\theta})$ coordinate system can be expressed in terms of the spherical wave functions in the (r, θ) coordinate system by applying the classical form of the translational addition theorem for bispherical coordinates.[20] Using the addition theorem, the total velocity potential expressed in the origin coordinate system can be written as

$$\begin{aligned}\phi_{\mathrm{total}} = \phi_0 \mathrm{e}^{-\mathrm{i}\omega t} \Bigg\{ & \sum_{n=0}^{\infty} (2n+1)\, g_n \mathrm{i}^n j_n(kr) P_n(\cos\theta) \\ & \times \left[1 + R_{\mathrm{s}_1}(-1)^n \mathrm{e}^{\mathrm{i}2kd_1} + R_{\mathrm{s}_2}(-1)^n \mathrm{e}^{\mathrm{i}2kd_2}\right] \\ & + \sum_{n=0}^{\infty} (2n+1)\, g_n \mathrm{i}^n h_n^{(1)}(kr) P_n(\cos\theta) \\ & + R_{\mathrm{s}_1} \sum_{n=0}^{\infty} \sum_{m=0}^{\infty} (2m+1)\, g_m \mathrm{i}^m (-1)^m \\ & \times a_m Q_{mn} j_n(kr) P_n(\cos\theta) \\ & + R_{\mathrm{s}_2} \sum_{n=0}^{\infty} \sum_{m=0}^{\infty} (2m+1)\, g_m \mathrm{i}^m (-1)^m \\ & \times a_m Q_{mn} j_n(kr) P_n(\cos\theta) \Bigg\}. \end{aligned} \tag{14}$$

The parameter Q_{mn} can be obtained from Ref. [21].

According to the correlation between the velocity potential and the particle velocity, we can also obtain

$$\begin{aligned} v_{\mathrm{total}} = \phi_0 \mathrm{e}^{-\mathrm{i}\omega t} \Bigg\{ & \sum_{n=0}^{\infty} (2n+1)\, g_n \mathrm{i}^n k j_n'(kr) P_n(\cos\theta) \\ & \times \left[1 + R_{\mathrm{s}_1}(-1)^n \mathrm{e}^{\mathrm{i}2kd_1} + R_{\mathrm{s}_2}(-1)^n \mathrm{e}^{\mathrm{i}2kd_2}\right] \\ & + \sum_{n=0}^{\infty} (2n+1)\, g_n \mathrm{i}^n k h_n^{(1)'}(kr) P_n(\cos\theta) \\ & + R_{\mathrm{s}_1} \sum_{n=0}^{\infty} \sum_{m=0}^{\infty} (2m+1)\, g_m \mathrm{i}^m (-1)^m \\ & \times a_m Q_{mn} k j_n'(kr) P_n(\cos\theta) \\ & + R_{\mathrm{s}_2} \sum_{n=0}^{\infty} \sum_{m=0}^{\infty} (2m+1)\, g_m \mathrm{i}^m (-1)^m \\ & \times a_m Q_{mn} k j_n'(kr) P_n(\cos\theta) \Bigg\}, \end{aligned} \tag{15}$$

where m is a dummy index of summation.

Equation (12) can also be written as

$$\begin{aligned}\phi_{\mathrm{total}} = \phi_0 \mathrm{e}^{-\mathrm{i}\omega t} \Bigg\{ & \sum_{n=0}^{\infty} (2n+1) A_n g_n \mathrm{i}^n j_n(kr) P_n(\cos\theta) \\ & + \sum_{n=0}^{\infty} (2n+1)\, a_n g_n \mathrm{i}^n h_n^{(1)}(kr) P_n(\cos\theta) \Bigg\}, \end{aligned} \tag{16}$$

where

$$\begin{aligned} A_n = {} & 1 + R_{\mathrm{s}_1} \mathrm{e}^{\mathrm{i}2kd_1} (-1)^n + R_{\mathrm{s}_2} \mathrm{e}^{\mathrm{i}2kd_2} (-1)^n \\ & + \frac{R_{\mathrm{s}_1}}{(2n+1)\, g_n \mathrm{i}^n} \sum_{m=0}^{\infty} (2m+1)(-1)^m g_m \mathrm{i}^m Q_{mn} \\ & + \frac{R_{\mathrm{s}_2}}{(2n+1)\, g_n \mathrm{i}^n} \sum_{m=0}^{\infty} (2m+1)(-1)^m g_m \mathrm{i}^m Q_{mn}. \end{aligned} \tag{17}$$

The sound scattering coefficients depend on the corresponding boundary conditions. For a rigid sphere, the boundary condition can be expressed as

$$\left.\frac{\partial \phi_{\mathrm{total}}}{\partial r}\right|_{r=a} = 0. \tag{18}$$

From Eqs. (13) and (15), we can obtain the numerical solution of scattering coefficients using the iterative method.

However, for a fluid sphere, equation (14) does not work due to the existence of refraction wave filling in the sphere. In this case, the boundary condition requires that the sound pressure and the radial velocity are continuous at the surface of the sphere, which can be expressed as

$$\begin{aligned} p|_{r=a} &= p_1|_{r=a}\,, \\ v|_{r=a} &= v_1|_{r=a}\,. \end{aligned} \tag{19}$$

Here, we can easily obtain the expressions of sound pressure and particle velocity according to their correlation with the velocity potential function. Similarly, by means of the iterative method, we can calculate the scattering coefficients.

2.3. Acoustic radiation force on a sphere between two boundaries

Once an object is placed in a harmonic continuous sound field, it will experience a mean force, known as the acoustic radiation force. The general formula of the force has already been given as[6]

$$\begin{aligned} \langle \boldsymbol{F} \rangle = &-\left\langle \iint_{S_0} \rho_0 \left(v_{\rm n} n + v_{\rm t}\right) {\rm d}s \right\rangle + \left\langle \iint_{S_0} \frac{\rho_0}{2} |v|^2 n {\rm d}s \right\rangle \\ &- \left\langle \iint_{S_0} \frac{\rho_0}{2c_o^2} \dot{\phi}^2 n {\rm d}s \right\rangle, \end{aligned} \tag{20}$$

where $v_{\rm n}$ and $v_{\rm t}$ are the normal and tangential components of the particle velocity, respectively. S_0 is the surface of the target at its equilibrium position.

In our model, the radiation force has only one component that lies perpendicular to the impedance boundary, called as the axial component. For oblique incidence, another component exists, which is parallel to the boundary. Here, we only need to consider the axial component. In the axial direction of wave motion, the acoustic radiation force on the sphere can be represented as[11,12]

$$\langle F_x \rangle = \langle F_r \rangle + \langle F_\theta \rangle + \langle F_{r\theta} \rangle + \langle F_{\rm t} \rangle\,, \tag{21}$$

where $\langle F_r \rangle$, $\langle F_\theta \rangle$, $\langle F_{r\theta} \rangle$, and $\langle F_{\rm t} \rangle$ are the force components listed as

$$\begin{aligned} \langle F_r \rangle &= -\frac{1}{2}\rho_0 a \left\langle \int_0^{2\pi} \left(\frac{\partial \psi}{\partial r}\right)^2_{r=a} \cos\theta \, {\rm d}\theta \right\rangle, \\ \langle F_\theta \rangle &= \frac{\rho_0}{2a} \left\langle \int_0^{2\pi} \left(\frac{\partial \psi}{\partial \theta}\right)^2_{r=a} \cos\theta \, {\rm d}\theta \right\rangle, \\ \langle F_{r\theta} \rangle &= \rho_0 \left\langle \int_0^{2\pi} \left(\frac{\partial \psi}{\partial \theta}\right)_{r=a} \left(\frac{\partial \psi}{\partial \theta}\right)_{r=a} \sin\theta \, {\rm d}\theta \right\rangle, \\ \langle F_{\rm t} \rangle &= -\frac{a\rho_0}{2c^2} \left\langle \int_0^{2\pi} \left(\frac{\partial \psi}{\partial t}\right)^2_{r=a} \cos\theta \, {\rm d}\theta \right\rangle. \end{aligned} \tag{22}$$

After some mathematical manipulation, the mean acoustic radiation force is expressed as[11,12]

$$\langle F_x \rangle = Y_{\rm p} S_{\rm c} \langle E \rangle\,, \tag{23}$$

where $\langle E \rangle = \frac{1}{2}\rho_0 k^2 \phi_0^2$ is the energy density of the incident wave, and $S_{\rm c} = \pi a^2$ is the cross-sectional area. The dimensionless factor $Y_{\rm p}$ is known as the radiation force function, which represents the radiation force per unit energy density and unit cross-sectional surface. Substituting Eq. (18) into Eq. (22), $Y_{\rm p}$ is expressed as

$$\begin{aligned} Y_{\rm p} = &-\frac{4}{(ka)^2} \sum_{n=0}^{\infty} (n+1) \left\{ {\rm Re}\left(g_n g_{n+1}^*\right) \left(\xi_{n+1}^{(1)} \xi_n^{(2)} + \xi_n^{(1)} \xi_{n+1}^{(2)} \right.\right. \\ &+ \eta_{n+1}^{(1)} \eta_n^{(2)} + \eta_n^{(1)} \eta_{n+1}^{(2)} + 2\xi_{n+1}^{(2)} \xi_n^{(2)} + 2\eta_n^{(2)} \eta_{n+1}^{(2)} \Big) \\ &+ {\rm Im}\left(g_n g_{n+1}^*\right) \left(\xi_{n+1}^{(2)} \xi_n^{(1)} + \xi_{n+1}^{(1)} \xi_n^{(2)} - \xi_n^{(1)} \eta_{n+1}^{(2)} \right. \\ &\left.\left. + \xi_n^{(2)} \eta_{n+1}^{(1)} + 2\xi_n^{(2)} \eta_{n+1}^{(2)} - 2\xi_{n+1}^{(2)} \eta_n^{(2)} \right) \right\}, \end{aligned} \tag{24}$$

where

$$\begin{aligned} \xi_n^{(1)} &= {\rm Re}\left[A_n\right], \quad \eta_n^{(1)} = {\rm Im}\left[A_n\right], \\ \xi_n^{(2)} &= {\rm Re}\left[a_n\right], \quad \eta_n^{(2)} = {\rm Im}\left[a_n\right], \end{aligned} \tag{25}$$

where Re and Im indicate the real and imaginary parts of a complex, respectively.

3. Simulation results

To illustrate the acoustic radiation force more intuitively, the numerical examples are provided in this section. We consider the axial acoustic radiation force acting on a sphere between two impedance boundaries. To simplify the issue, we assume that the reflecting coefficients of two boundaries are opposite numbers. The fluid sphere in our simulation is filled with oleic acid. Some acoustic parameters that may be used in the simulation are listed in Table 1.[11]

Table 1. Some physical parameters used in the simulations.

Material	Density /(kg/m^3)	Compressible velocity/(m/s)
Water	1000	1480
Oleic acid	938	1450

3.1. Radiation force on the sphere with no boundary

First, $Y_{\rm p}$ for a rigid sphere and a fluid oleic acid sphere without any reflecting boundary in an on-axis Gaussian beam is presented here to verify the correctness of the formulation we deduced above. Considering the weakening weight of high-order terms, we truncate the expression at $n = 60$ to achieve a good approximation. The results are shown in Figs. 2(a) and 2(b) respectively. They are in good agreement with those in Ref. [5]. The inspection of Fig. 2 reveals that for a rigid sphere, $Y_{\rm p}$ notably increases when $ka < 1$ for different beam waists. Actually, when $ka < 1$, we can judge the sign of radiation force function through elementary principles. All of the curves have a fluctuation around $ka = 2$. Besides, the influence of the beam waist on $Y_{\rm p}$ becomes small as the beam waist increases. When the beam waist is much greater than

the wavelength, the curve will approach the one in a plane incident wave. For an oleic acid, there are a series of peaks and dips when $ka > 2$, which is caused by the effects of resonant vibration of the sphere. Similarly, Y_p decreases on the whole when the beam waist is small. As W_0 increases, the curve approaches that in the plane wave.

Another critical parameter of a Gaussian beam is the scale length $L_0 = kW_0^2$. In this paper, L_0 is always selected as a certain multiple of wavelength. Thus, for a certain value of W_0, L_0 is also several times of the wavelength. In other words, the ratio of L_0 to the radius of sphere completely depends on the frequency of the sound.

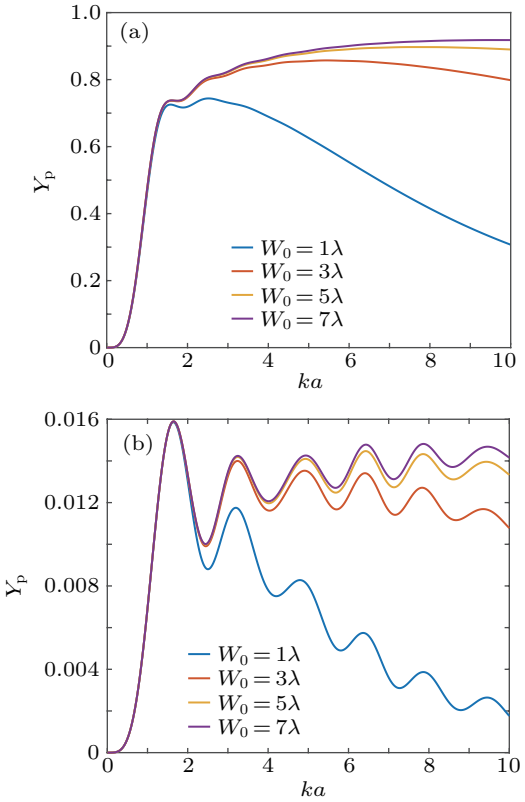


Fig. 2. The Y_p curves versus ka for a sphere without reflecting boundary. (a) Rigid sphere; (b) oleic acid sphere.

3.2. Radiation force on a sphere near one boundary

Then, we consider the acoustic radiation force function on the sphere near an impedance boundary in an on-axis Gaussian beam whose beam waist $W_0 = 3\lambda$. The distance between the sphere and boundary is set as twice the radius of the sphere. The results for a rigid sphere and a fluid oleic sphere are shown in Figs. 3(a) and 3(b), respectively. Similar results for cylindrical particles are exhibited in Ref. [12].

It is very interesting to find that whether it is the rigid or fluid sphere, the acoustic radiation force is positive or negative, depending on the value of ka. It is worth mentioning that when Y_p is negative, it means that the particle is pulled toward the acoustic source. Also, Y_p becomes more oscillatory when the boundary is added due to the interaction of the scattering wave from the real and image sphere and the reflection wave from the impedance boundary. The amplitude of Y_p increases as the reflecting coefficient of the boundary accrues. It is also worth mentioning that the position of the peaks and dips of the curves are not obviously affected by changing the reflecting coefficient of the impedance boundary.[11,12]

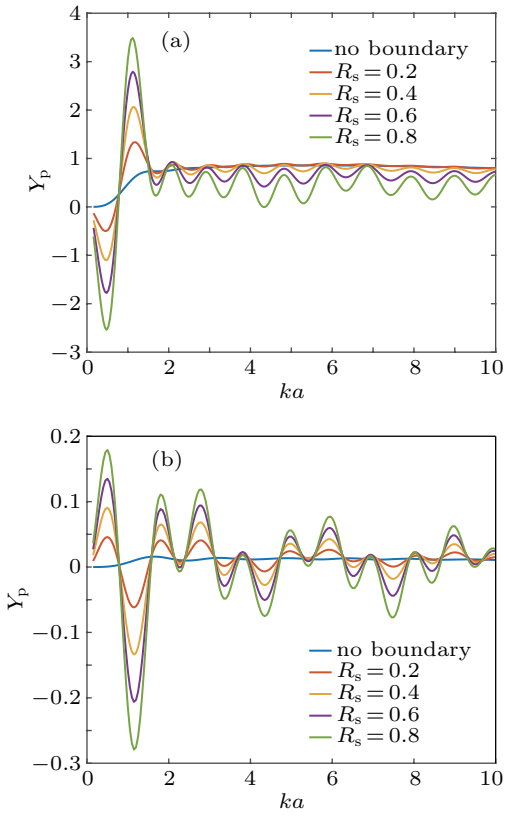


Fig. 3. The Y_p curves versus ka for a sphere near one impedance boundary with different reflecting coefficients. (a) Rigid sphere; (b) oleic acid sphere.

Till now, we have not considered how the distance between sphere and boundaries influences the acoustic radiation force in this issue. To further study the effects of impedance boundary, the radiation force functions of a rigid sphere are simulated in the range of $2 < d/a < 10$, where d represents the distance between sphere and boundary. The acoustic reflecting coefficient and the dimensionless parameter are respectively set as $R_s = 0.5$ and $ka = 0.5$. Only one boundary exists near the sphere in this case and the beam waist of the incident Gaussian beam is still 3λ. The corresponding result is presented in Fig. 4.

By inspecting the simulating result, we can find that they are very similar to sine curves in shape. All these curves have the same period. It is due to the existence of complex exponential function in our previous induction. In addition, the larger reflecting coefficient will generate higher amplitude of the acoustic radiation force. This can be expected from our previous discussion since only the independent variable is changed.

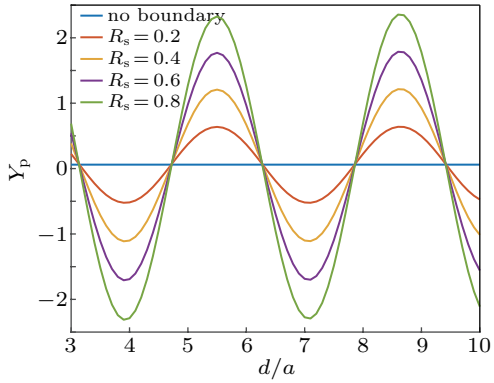


Fig. 4. The Y_p curves versus d/a for a rigid sphere near an impedance boundary when $ka = 0.5$.

In all our previous simulations, the beam waist of Gaussian beam is always set as 3λ. Now the acoustic radiation force functions in Gaussian beams with different beam waists are considered. The reflecting coefficient is set as $R_s = 0.5$. Other parameters are exactly the same as before. For beam waists ranging from λ to 7λ, the result for a rigid sphere is shown in Fig. 5.

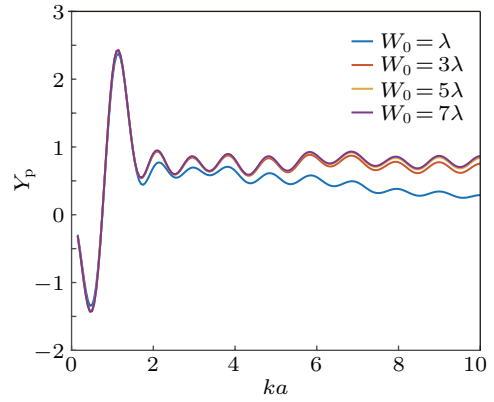


Fig. 5. The Y_p curves versus ka for a rigid sphere near one impedance boundary.

From the results we can find that the difference is mainly reflected at middle and high frequency. At low frequency, the curves nearly coincide with each other. As the beam waist of Gaussian beam increases, the amplitude of negative acoustic radiation force is becoming larger. As for the positive acoustic radiation force, the difference is minor. Predictably, with the increase of the beam waist, the curve will approach that in the field of plane incident wave.

3.3. Radiation force on a sphere between two boundaries

To study the effects of two impedance boundaries on Y_p, we consider a sphere between two boundaries, the distances of which from the center of sphere are respectively $2a$ and $6a$. The incident wave is still an on-axis Gaussian beam whose beam waist is 3λ. The results of the computation of the acoustic radiation force function with different acoustic reflecting coefficients are shown in Figs. 6(a) and 6(b).

Figure 6(a) presents the results for a sphere between two impedance boundaries with different reflecting coefficients. Compared with the curves in Fig. 3(a), we can find that adding another boundary can cause much difference to the acoustic radiation function. It is surprising that the amplitude of Y_p at middle and high frequency is much larger than that at low frequency. When ka is around 8, we can even obtain such a large negative force that the value of Y_p reaches 50. In addition, the positions of the peaks and dips also change a lot. All of these phenomena reflect the huge influence of adding one more boundary to the original model, as we need to consider the interaction between six kinds of waves existing in the whole space now. Figure 6(b) shows the results for an oleic acid sphere. It reveals that the peaks and dips are much denser compared with that in Fig. 3(b), and the amplitude is much larger whether the frequency is low or high. These peaks and dips arise from the more complex resonant vibration within the sphere near two boundaries. It can also be concluded from Fig. 6 that increasing the reflecting coefficient still leads to more turbulent oscillation about Y_p. If the boundary is absolutely rigid, we can obtain large radiation force more easily regardless of the property of sphere.

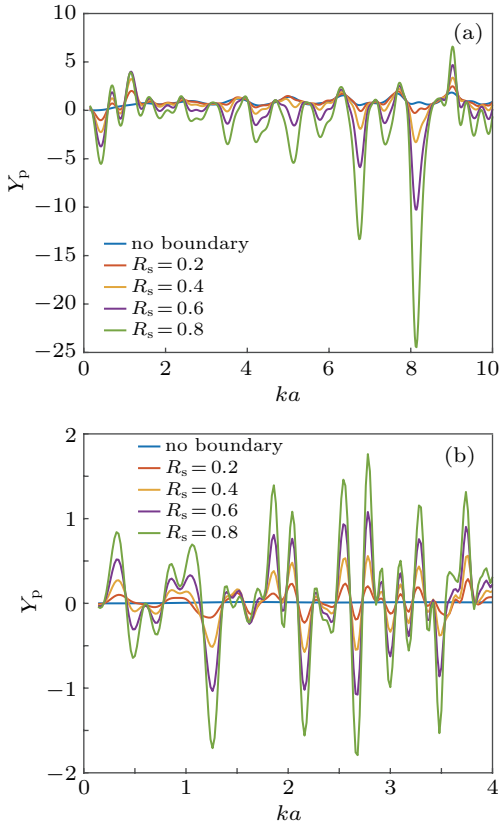


Fig. 6. The Y_p curves versus ka for a sphere between two impedance boundaries with different reflecting coefficients. (a) Rigid sphere; (b) oleic acid.

Now we turn to study the effects of the distance between two boundaries on the acoustic radiation force function. At this time, the distance between the center of sphere and the

first boundary is set as $d_1 = 2a$. Other parameters are exactly the same as the last simulation. The acoustic radiation force functions of a rigid sphere when d_2/a ranges from 2 to 20 are shown in Fig. 7. It is revealed that as the value of d_2/a increases, Y_p also fluctuates periodically with the period of around 6. However, it is interesting to find that the amplitudes of the positive and negative radiation force functions are no longer the same, or rather, it is more likely to obtain large negative than positive acoustic radiation force in this case. This kind of asymmetry is typically different from that when only one boundary exists.

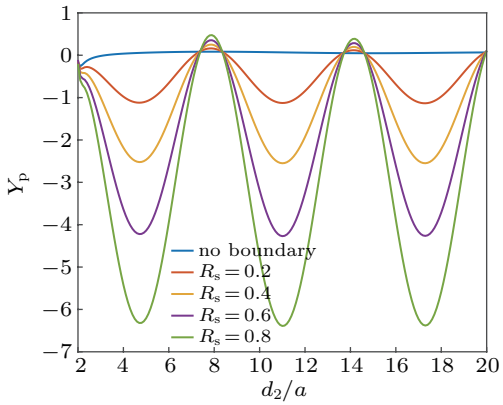


Fig. 7. The Y_p curves versus d_2/a for a rigid sphere between two impedance boundaries when $ka = 0.5$.

To further study the effect of two impedance boundaries on the acoustic radiation force of a particle placed in the sound field, we have simulated the radiation force function on a rigid sphere in the range of $0 < ka < 7$ and $2 < d/a < 10$. The reflecting coefficients of two boundaries are the same as above. The results are presented in Fig. 8. It is easy to find that the peaks and dips of the radiation force function are more densely packed with the increase of d/a. Negative radiation force can be acquired if ka is properly selected.

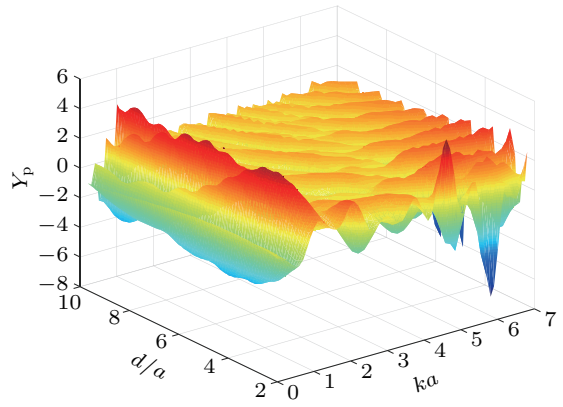


Fig. 8. The acoustic radiation force function versus ka for a rigid sphere between two boundaries at different values of d/a.

Similarly, now we study the acoustic radiation force functions in Gaussian beams with different beam waists. Other parameters are not changed compared with the corresponding simulations in Section 3.2. The results are presented in Fig. 8. It is not hard to find that the values of beam waists only evidently affect the curves at middle and high frequency, which is similar to that near one boundary. When ka is relatively small, all the curves nearly coincide with each other. When the beam waist increases to a certain extent, the curve is very close to that in the field of plane wave.

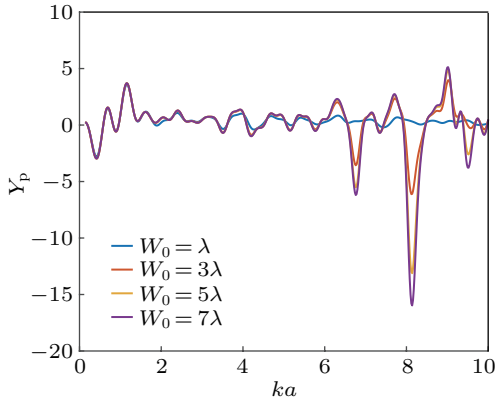


Fig. 9. The Y_p curves versus ka for a rigid sphere between two impedance boundaries.

4. Conclusion and perspective

Based on the study of acoustic radiation force in free space and near one boundary, the acoustic radiation force acting on the sphere between two impedance boundaries is derived in this work. Applying the translation addition theorem for bispherical coordinates and finite series method, we successfully compute the acoustic radiation force function with different reflecting coefficients in this case. We analyze the characteristic of acoustic radiation force for both rigid and fluid spheres between two boundaries in detail and verify the possibility to obtain large negative acoustic radiation force at a relatively higher frequency. Besides, the influences of the distances between sphere and boundaries are also discussed here according to the simulation results. Furthermore, as the most important parameter of a Gaussian beam, the value of the beam waist also plays a critical role in the acoustic radiation force, which mainly affects the curves at high frequency. As the beam waist increases, the acoustic radiation force gradually approaches that in the field of plane incident wave. In conclusion, our study provides a theoretical guidance for the acoustic manipulation and drug delivery in biomedical ultrasound and other fields. However, if further progress can be made in the radiation force, such as taking the viscosity of fluid medium into account, more valuable and meaningful results can be obtained based on the present paper.

References

[1] Wu J R 1991 *J. Acoust. Soc. Am.* **89** 2140

[2] Lee J, Teh S Y, Lee A, Kim H H, Lee C and Shung K K 2009 *Appl. Phys. Lett.* **95** 073701
[3] Lee J, Teh S Y, Lee A, Kim H H, Lee C and Shung K K 2010 *Ultrasound Med. Biol.* **36** 350
[4] King L V 1934 *Proc. Roya. Soc. London* **147** 212
[5] Wu J R and Du G H 1990 *J. Acoust. Soc. Am.* **87** 997
[6] Yosioka K and Kawasima Y 1955 *Acta Acust. United. Ac.* **5** 167
[7] Awatani J 1955 *J. Acoust. Soc. Am.* **27** 278
[8] Hasegawa T and Yosioka K 1969 *J. Acoust. Soc. Am.* **46** 1139
[9] Hasegawa T 1979 *J. Acoust. Soc. Am.* **65** 32
[10] Azarpeyvand M and Azarpeyvand M 2013 *J. Sound Vib.* **332** 2338
[11] Qiao Y P, Zhang X F and Zhang G B 2017 *J. Acoust. Soc. Am.* **141** 4633
[12] Qiao Y P, Zhang X F and Zhang G B 2017 *Wave Motion.* **74** 182
[13] Huang H and Guanauard G C 1997 *Int. J. Solids Structures.* **34** 591
[14] Miri A K and Mitri F G 2011 *Ultrasound in Med. & Bio.* **37** 301
[15] Kogekink H and Li T 1966 *Appl. Optics.* **5** 1550
[16] Marston P L 2011 *J. Acoust. Soc. Am.* **129** 1773
[17] Marston P L 2011 *J. Acoust. Soc. Am.* **130** 1091
[18] Gaunaurd G C and Huang H 1994 *J. Acoust. Soc. Am.* **96** 2526
[19] Morse P M and Ingard K U 1968 *Theoretical Acoustics* (New York: McGraw–Hill) p. 401
[20] Friedman B and Russek J 1954 *Quart Appa Math.* **12** 13
[21] Gaunaurd G C and Huang H 1996 *IEEE Trans. UFFC* **43** 690